Current Clinical Pharmacology, 2019, *14*, 132-140

RESEARCH ARTICLE

Rabbit as an Animal Model for Pharmacokinetics Studies of Enteric Capsule Contains Recombinant Human Keratinocyte Growth Factor Loaded Chitosan Nanoparticles

Palanirajan V. Kumar[1,*], Marwan A. Abdelkarim Maki[1], Yeong S. Wei[1], Lee M. Tatt[1], Manogaran Elumalai[1], Shiau-Chuen Cheah[2], Bharathy Raghavan[1] and Abu Bakar Bin A. Majeed[3]

[1]*Department of Pharmaceutical Sciences, UCSI University, Jalan Menara Gading 1, Taman Connaught, Wilayah Persekutuan Kuala Lumpur, 56000 Malaysia;* [2]*Department of Medicine & Health Science, UCSI University, Jalan Menara Gading, UCSI Heights, Cheras, Kuala Lumpur, 56000 Selangor Malaysia;* [3]*Department of Pharmacy, Universiti Teknologi MARA, Bandar Puncak Alam, 42300 Selangor Malaysia*

Abstract: ***Background*:** Recombinant human keratinocyte growth factor (rHuKGF) has gained considerable attention by researchers as epithelial cells proliferating agent. Moreover, intravenous truncated rHuKGF (palifermin) has been approved by Food and Drug Administration (FDA) to treat and prevent chemotherapy-induced oral mucositis and small intestine ulceration. The labile structure and short circulation time of rHuKGF *in-vivo* are the main obstacles that reduce the oral bioactivity and dosage of such proteins at the target site.

***Objective*:** Formulation of methacrylic acid-methyl methacrylate copolymer-coated capsules filled with chitosan nanoparticles loaded with rHuKGF for oral delivery.

***Methods*:** We report on chitosan nanoparticles (CNPs) with diameter < 200 nm, prepared by ionic gelation, loaded with rHuKGF and filled in methacrylic acid-methyl methacrylate copolymer-coated capsules for oral delivery. The pharmacokinetic parameters were determined based on the serum levels of rHuKGF, following a single intravenous (IV) or oral dosages using a rabbit model. Furthermore, fluorescent microscope imaging was conducted to investigate the cellular uptake of the rhodamine-labelled rHuKGF-loaded nanoparticles. The proliferation effect of the formulation on FHs 74 Int cells was studied as well by MTT assay.

***Results*:** The mucoadhesive and absorption enhancement properties of chitosan and the protective effect of methacrylic acid-methyl methacrylate copolymer against rHuKGF release at the stomach, low pH, were combined to promote and ensure rHuKGF intestinal delivery and increase serum levels of rHuKGF. In addition, *in-vitro* studies revealed the protein bioactivity since rHuKGF-loaded CNPs significantly increased the proliferation of FHs 74 Int cells.

***Conclusion*:** The study revealed that oral administration of rHuKGF–loaded CNPs in methacrylic acid-methyl methacrylate copolymer-coated capsules is practically alternative to the IV administration since the absolute bioavailability of the orally administered rHuKGF–loaded CNPs, using the rabbit as animal model, was 69%. Fluorescent microscope imaging revealed that rhodamine-labelled rHuKGF-loaded CNPs were taken up by FHs 74 Int cells, after 6 hours' incubation time, followed by increase in the proliferation rate.

ARTICLE HISTORY

Received: April 04, 2018
Revised: November 01, 2018
Accepted: November 13, 2018

DOI:
10.2174/1574884714666181120103907

Keywords: Recombinant human keratinocyte growth factor, chitosan nanoparticles, proliferation, fluorescence imaging, protein delivery, pharmacokinetics, bioavailability.

1. INTRODUCTION

Recombinant human keratinocyte growth factor is a signaling molecule that binds to fibroblast growth factor receptor (FGFR2b) and stimulates wounds healing through distinct expression patterns [1-4]. *In-vitro*, rHuKGF is a potent mitogen and acts as an important mesenchymal mediator for growth, differentiation and morphogenesis of a wide range of epithelial derived cells. It is noteworthy that rHuKGF expression is often linked to tissue expansion and wound repair [4]. In a variety of organs, targeted overexpression of rHuKGF *in-vivo* leads to hyperplasia of epithelial tissues [5]. Researchers reported an upregulation in cutane-

*Address correspondence to this author at the Department of Pharmaceutical Technology, Faculty of Pharmaceutical Sciences, UCSI University, 56000, Kuala Lumpur, Malaysia; Tel: +60103782399; Fax: (+603) 9102 2614; E-mail: vijayarajkumar_p@yahoo.com

2212-3938/19 $58.00+.00

ous wounds that are associated with rHuKGF expression which accelerates the repair process [6] and stimulate the thickening of the gastrointestinal tract (GIT) [7]. In addition, rHuKGF has been widely used for malignant patients under radio and chemotherapy to treat oral mucositis. Patients undergoing high dose chemotherapy followed by hematopoietic stem cell transplantation (HSCT) were prone to development oral mucositis. Palifermin, a FDA approved truncated rHuKGF, is being used for the prevention of severe oral mucositis. The clinical response to palifermin was related to mucosal epithelial protection, epithelial proliferation, apoptosis inhibition of epithelial cell, acceleration of immune reconstitution, inhibition of graft-versus-host disease in patients undergoing HSCT and reducing the severity and duration of oral mucositis in patients undergoing radio or chemotherapy [8, 9]. Furthermore, pediatric patients with hematological malignancies undergoing HSCT can be treated by palifermin because it is the safest drug to treat severe mucositis. It has also been used as a prophylactic drug to prevent the development of oral mucositis in pediatric patients who are at high risk [10]. Studies revealed that the blood concentration of palifermin declines in the first 30 minutes after a single IV dose administration and after 1 to 4 hours, there is a slight increase in the concentration followed by a terminal decline phase. Palifermin has an extravascular distribution showing a linear pharmacokinetic. Whereas, the clearance was 2- to 4-fold higher and the volume of distribution was 2-fold higher when compared with healthy subjects. The elimination half-life ($t_{1/2}$) was 4.5 hours and was the same for the two groups of subjects [11].

Nanoparticles (NPs) drug delivery has attracted the attention of researchers as a potential targeting strategy for protein drugs for internal healing. Human cells like intestinal epithelial cells are quite permeable to macromolecules and nanocarriers [12-14]. Active and passive mechanisms are the two major strategies for cell-specific targeting with NPs. Active mechanism depends on the interaction between receptors on the target cell and NPs. On the other hand, passive mechanism involves an increase in vascular permeability and maintains long-circulation of NPs at the targeted sites [15]. In vascular permeability and retention, NPs clearance by mononuclear phagocyte system (MPS) and the characteristics of NPs are important concepts in NPs-based drug delivery. Nanoparticles characteristics have a critical role in drug delivery; particles size < 200 nm, smooth texture and spherical shape [16-18]. Chitosan-based NPs have gained considerable attention due to their ability to protect and facilitate cellular uptake of several biopharmaceuticals including genes, proteins and anticancer drugs. Moreover, chitosan-based delivery systems provide versatility with respect to mucosal delivery and can be administered through various routes including oral, nasal, and pulmonary [19-22]. Chitosan nanoparticles can be used to formulate oral delivery system for human growth factor. It was postulated that due to positive charges of the chitosan, it could adhere to the small intestinal mucosa, which has negative charges. In particular, this class of carrier holds tremendous promise in the areas of cancer therapy and controlled delivery of vaccines [23]. Chitosan as a mucoadhesive polymer has the potential to increase cellular permeability and improve the bioavailability of orally administered protein drugs. Recently, chitosan and poly gamma-glutamic acid were freeze-dried to produce pH-sensitive nanoparticles and filled inside Eudragit L100-55 enteric-coated capsule for oral delivery of insulin. This preparation has proven that insulin was retained in the acidic environment of the stomach for a long duration without degrading and successfully brought to the small intestine promoting the intestinal absorption of insulin and extending the duration for blood glucose reduction for as long as 15 hours [24].

The purpose of this study was to formulate methacrylic acid-methyl methacrylate copolymer-coated capsules and filled with chitosan nanoparticles loaded with rHuKGF for oral delivery. The pharmacokinetics parameters were determined using rabbit as animal model following single oral or IV administration of the prepared formulation. Furthermore, the effect on the proliferation of FHs 74 Int cells was investigated as well as the uptake of rHuKGF-loaded CNPs by these cells.

2. MATERIALS AND METHODS

2.1. Materials

Recombinant human keratinocyte growth factor (Sigma, USA), chitosan (Aldrich, Iceland), sodium tripolyphosphate (Sigma Aldrich, USA), trehalose (Merck, Germany), methacrylic acid-methyl methacrylate copolymer (1:1) 135,000 MW (Kollicoat MAE 100 P) (Sigma, Germany), KGF (FGF7) ELISA kit (abcam, UK), Rhodamine 6G (Sigma, Germany), Thiazolyl Blue Tetrazolium Bromide powder (MTT) (Sigma Aldrich, USA), DAPI (4',6-diamidino-2-phenylindole) (Sigma, Germany), FHs 74 Int (ATCC, USA), Hybri-Care Medium 46-X (ATCC, USA), GibcoTM Dulbecco's Modified Eagle's Medium (DMEM) (Thermo Fisher Scientific, USA) and veterinary capsules size 5 for rabbits (Torpac Inc., USA).

2.2. Preparation and Optimization of rHuKGF-loaded CNPs

The rHuKGF-loaded CNPs were prepared by ionic gelation method with modification, between low molecular weight chitosan and tripolyphosphate (TPP) [25]. Based on the optimization procedure designed by Fan *et al* [26]. After the preparation of NPs, 17.5 µL of trehalose (40 mg/ml) was added as a cryoprotectant [27]. The mixture was frozen in an ultra-low temperature freezer at –80 °C for 24 hours [28]. Finally, the frozen NPs were lyophilized using a freeze dryer and rHuKGF-loaded CNPs were obtained into powder form.

2.3. Characterization of Nanoparticles

The size, polydispersity index (PdI), and zeta potential of the prepared NPs were measured by Zeta Sizer. The morphological characteristics of CNPs were measured by field emission scanning electron microscope. To determine the loading capacity, rHuKGF-loaded CNPs were mixed with ultra-pure water then centrifuged 3000 rpm at 4 °C for 15 minutes, the amount of free rHuKGF was measured in the clear supernatant by KGF (FGF7) ELISA kit [29]. Finally, loading capacity was calculated according to the following equation:

$$Loading\ capacity = \frac{Total\ rHuKGF - Free\ rHuKGF}{Nanoparticles\ weight} \times 100$$

2.4. rHuKGF Content Analysis

ELISA test was used for quantitative determination of rHuKGF [30]. Samples were diluted when necessary based on the sensitivity of ELISA reader (FLUOstar Omega, BMG LABTECH, Germany). Finally, rHuKGF concentration was measured by mean optical density (O.D) values, recorded at 450 nm ± S.D, *n*=6.

2.5. Capsules Filling and Coating with Kollicoat MAE 100 P

Veterinary hard gelatin capsules size 5 (Body: 9.32 mm in length and 4.68 mm in diameter, Cap: 6.91 mm in length and 6.20 mm in diameter, for rabbit) were uniformly filled by appropriate capsules filling funnel (Torpac, X-5, USA) with 40 mg of loaded CNPs to obtain the required dose of rHuKGF along with lactose as a diluent. The prepared capsules were coated with Kollicoat MAE 100 P by dip coating method [31]. Briefly, capsules were held by forceps and dipped into the coating suspension (Kollicoat MAE 100 P 62.5 g, triethyl citrate 6.25 g, talc 26.25 g, titanium dioxide 5 g, acetone 342.9 g, isopropanol 514.2 g and water 42.9 g) in and out for fifteen times. The coating film was dried with a steam of warm air after each dip.

2.6. *In-vitro* Dissolution Studies

Dissolution studies of rHuKGF capsules were performed by USP dissolution test apparatus I (Basket apparatus) (Electro Lab, TDT08L) at 100 rpm, with 900 mL solution at 37 ± 0.5 °C [32]. Briefly, 6 capsules were placed in a 0.1M HCL solution for 2 hours and samples were collected every 30 minutes repeated to 2 hours. After 2 hours, the previous buffer was replaced by pH 5.5 buffer and the same procedure was repeated for 2 hours. Finally, pH 5.5 buffer was replaced by pH 7.4 phosphate buffer in each vessel where the capsules had maintained for 6 hours. The samples were analyzed for rHuKGF content by ELISA test.

2.7. Morphological Characterization and Cells Proliferation

Structural characterization of FHs 74 Int cells was observed under a light microscope (Axio Vert.A1, Carl Zeiss, Germany), and the cells count was measured by hemocytometer cells counting protocol. Cells proliferation was analyzed by MTT assay, as described by Mosmann [33]. Briefly, cells were seeded in 96-well plates in 100 µL of culture medium at a density of $1x10^4$ cells/well and grown for 24 hours in culturing medium. The cells were then washed 3 times with PBS, then treated with 100 µL of CNPs prepared in Hybri-Care Medium, rHuKGF solutions with concentrations from 10 to 50 ng/mL and rHuKGF-loaded CNPs solutions with concentrations from 10 to 50 ng/mL (positive control). The plates were then incubated at 37°C, 5% CO2 and 90 % humidity for 24 hours after which 10 µL of MTT reagent was added directly into each well. The plates were then incubated for additional 3 hours under same atmospheric conditions until purple precipitate was visible and 100 µL of the detergent reagent was added, then the plates were incubated at room temperature in the dark for 2 hours. The optical density was measured at 570 nm using a spectrophotometric microtiter plate reader (FLUOstar Omega, BMG LABTECH, Germany) against blank wells, with only DMEM, to subtract background absorbance at 690 nm. Cells incubated with DMEM without CNPs were used as a negative control [33-37].

2.8. Preparation of Rhodamin 6G-labeled rHuKGF-CNPs

Freeze-dried rHuKGF-CNPs were re-dispersed in 5 mL dimethyl sulfoxide solution followed by the addition of 0.5 mL NaOH (0.1 M) and rhodamine 6G was dissolved in methanol at 10.0 mg/mL concentration. The reaction was allowed to proceed for 4 hours in the dark at room temperature [38]. The prepared rhodamine-labeled rHuKGF-CNPs were centrifuged and washed several times with methanol until the free rhodamine 6G could not be detected in the supernatant. Then NPs were separated by centrifugation and resuspend in 5 mL phosphate-buffered saline (PBS).

2.9. Fluorescence Microscopy Imaging for Cellular Uptake Assessment of rHuKGF-CNPs

A Zeiss Axio Vert.A1 inverted microscope (Carl Zeiss, Germany) equipped with HBO 50 W mercury vapor lamp and exciter/emitter filter combinations was used. Filter 43 (550 nm excitation and 573 nm emission) to observe rhodamine-labeled CNPs and filter 49 (359 nm excitation and 457 nm emission) to observe DAPI-stained cells. Cells were seeded at $1x\ 10^5$ cells/well. Cells were then transferred to microtubes and the growth medium was then changed to serum-free medium supplemented with rhodamine-labeled rHuKGF-loaded CNPs (100 µg/mL) and incubated for 6 hours. Immediately after incubation, the cells were washed with PBS and fixed by 100 µL of 37% formaldehyde then incubated for 10 minutes at room temperature followed by further washing steps. Cells were separated with centrifugation at 3000 rpm and the supernatant was removed, then 10 µL of DAPI stain (1 µg/ml) was added. The cells were incubated in the dark for 20 minutes. Then cells were separated, suspended in 20 µL of PBS and 1 µL of this suspension was placed onto a glass slide, then sealed with a coverslip. Images were captured, under standardized setting and exposure time, by fluorescent microscope and Zen 2012 software (Blue Edition) was used for images analysis.

2.10. Pharmacokinetic Parameters

The population was comprised of 9 females, 12-week-old, New Zealand white rabbits (Oryctolagus cuniculi; One Stop Rabbit Farm and Trading, Selangor, Darul Ehsan, Malaysia) with average weight of 1.5 ± 0.1 kg. All the methods were performed in accordance with the guidelines and experimental protocols approved by ethics committee of Faculty Research and Scholarly Activity (FRSA), Faculty of Pharmaceutical Sciences, UCSI University Animal Care and Use Committee (Ref: UCSI/Pharmacy/2014/FRGS/Approval/01). The rabbits were divided into 3 groups of each *n*=3, group 1 animals given placebo as a control, whereas group 2, fasted animals, was given a formulation of rHuKGF

(60 µg/kg) by IV injection. Group 3, fasted rabbits, was received an equivalent dose of lyophilized rHuKGF-loaded CNPs filled into capsules size 5 coated with methacrylic acid-methyl methacrylate copolymer. The capsule was administered through oral wooden gag with a central opening of 9 mm diameter. The capsules were placed deep into the throat through the opening and immediately 20 mL of water was given by a syringe to facilitate swallowing of the capsule intact and to prevent it from sticking to the animal's throat. After local anesthesia of ears with a topical lidocaine–prilocaine cream (EMLA, AstraZeneca, Wayne, PA), samples, 0.5 ml, of blood were collected in serum separator-tubes before and after rHuKGF dosage from 0 to 16 hours. After clot formation, the tubes were centrifuged at 2000 rpm for 10 minutes at 20°C using Beckman centrifuge. The serum was separated and stored at -80°C for further analysis. The amount of rHuKGF present in the serum was determined by KGF (FGF7) ELISA kit. The area under the serum rHuKGF *versus* time curves (AUC0-16 hours) following the IV injection of rHuKGF, and oral administration of rHuKGF-loaded CNPs capsules was calculated using the linear trapezoidal rule. The elimination rate constant, t1/2, apparent volume of distribution (Vd), clearance (Cl) and absolute bioavailability (%*F*) were measured as well.

2.11. Data Analysis

Each experiment was performed independently in triplicate at least. Statistical analysis was performed by GraphPad Prism Software 7.0c (La Jolla, CA). For cellular uptake and proliferation studies, the difference between each group was tested by two-way ANOVA analysis of variance, followed by the Dunnett's multiple comparisons test for between-group comparisons. Animals' grouping was performed in a randomized manner. The pharmacokinetic data were calculated using Pharmacological Calculation System, version 4.2 by Springer Verlag, USA. The statistical analysis of the difference between each group was tested by one-way ANOVA, followed by the Post hoc test for between-group comparisons. All Results are presented as mean ± SD. Statistical significance was defined as follows: $*P < 0.05$, $**P < 0.01$, $***P < 0.001$, $****P < 0.0001$. Significance was accepted at $P < 0.05$.

3. RESULTS AND DISCUSSION

3.1. Preparation and Optimization of rHuKGF-loaded CNPs

The rHuKGF-loaded CNPs were prepared based on ionic gelation method. Parameters such as concentration, pH and temperature of chitosan solution were optimized. In addition, the concentration and the temperature of tripolyphosphate (TPP) solution and the ratio between chitosan and TPP (1:3.3) were optimized as well [39]. Initially, rHuKGF-loaded CNPs were prepared without cryoprotectant. During lyophilization process, the prepared NPs were aggregated. Therefore, trehalose was added as a cryoprotectant to prevent NPs aggregation during the formation process.

3.2. Characterization of Nanoparticles

According to our previous reports [39, 40], the produced rHuKGF-loaded CNPs were spherical, colorless, cloudy, positively charged and in a monodisperse system with a particles size of 119 ± 74.62 nm, surface charge of +20.3 ± 6.46 mV and 0.217 PdI. The loading capacity of the prepared CNPs was found to be 93.3 ± 2.02%. Continuous monitoring and detection system was designed as well to detect the formation of CNPs and measure the amount of TPP required to convert all chitosan molecules presented in the solution into NPs.

3.3. Weight Determination of Capsules Filled with rHuKGF-loaded CNPs

The weight of 6 empty capsules was measured as well as the amount of rHuKGF-loaded CNPs and lactose that filled. The results as mean weight ± S.D are shown in Table **1**.

Table 1. Results of average weight of capsules containing the required rabbit dose of rHuKGF (60 µg/kg).

Material	Mean Weight ± S.D (mg)*
Empty capsule	28.87 ± 0.73
rHuKGF-loaded CNPs**	39.23 ± 3.72
Trehalose	0.70 ± 0.16
Lactose	91.17 ± 3.27
Filled capsule	159.97 ± 2.22

*Data are expressed as mean weight ± S.D (n=6).
**The weight of CNPs that containing 90 µg of rHuKGF for rabbits with average weight of 1.5 kg.

3.4. *In-vitro* Dissolution Studies

Dissolution studies results revealed that the methacrylic acid-methyl methacrylate copolymer-coated capsules prevented the release of rHuKGF at pH 1.2, simulated stomach pH, Fig. (**1**). Once the coated capsules that filled with rHuKGF-loaded CNPs placed into medium with pH >5.5, simulated small intestine pH, the coating film started to dissolve and allowed the release of rHuKGF up to 70% within 4 hours and in pH 7.4 the cumulative percentage release has reached 89.5% within 6 hours. Whereas, the pure rHuKGF reached the higher release of 98.7% within the first 30 minutes at gastric pH and start to decrease gradually, this is mainly due to acidic degradation [41].

3.5. Cell-lines Studies

Light microscope images show the characteristic morphology of FHs 74 Int cells, such as oval shaped nucleus and an adherent epithelial cell type (Fig. **2**). The viability of the FHs 74 Int cells according to MTT assay before and after exposure to rHuKGF-loaded CNPs, rHuKGF and CNPs only is shown in Fig. (**3**). There was a significant increase observed in the percentage cell viability of FHs 74 Int cells when exposed to rHuKGF-loaded CNPs and rHuKGF only at a concentration of 50 ng/ml, $p < 0.05$. The findings, therefore, indicated that CNPs are not cytotoxic to the cell lines investigated. The MTT assay results confirmed that CNPs could deliver the loaded rHuKGF to the intercellular compartments

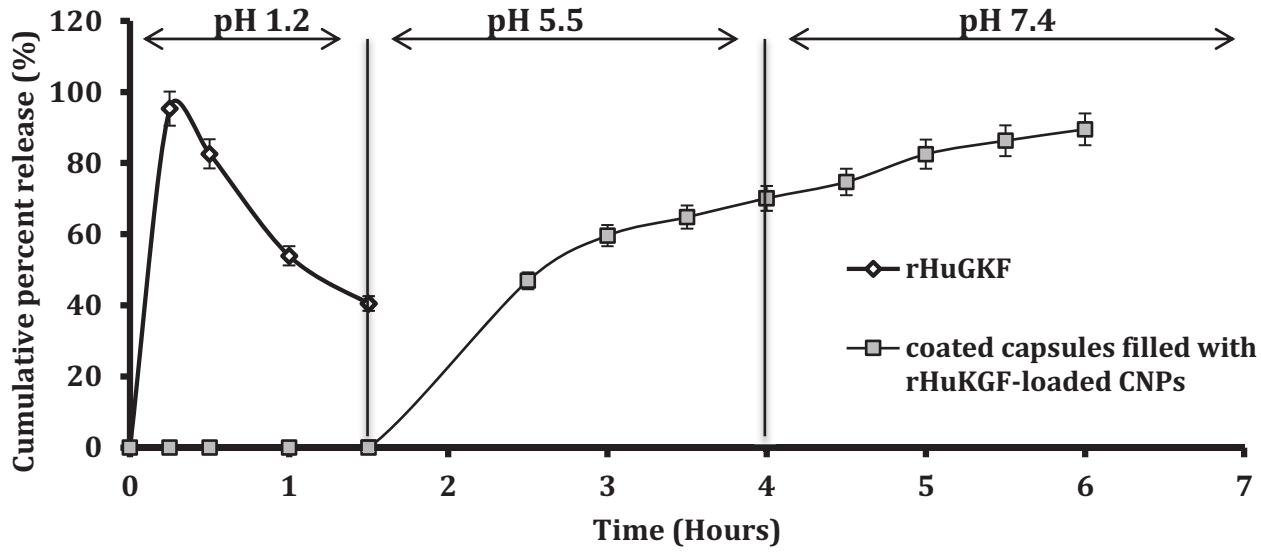

Fig. (1). Graph shows the release behavior of rHuKGF in 3 buffer media with pH 1.2, 5.5 and 7.4. Data are expressed as mean ± S.D (n=6). The release of pure rHuKGF was 98.7 % at pH 1.2 within 15 minutes and decreased to 40.5 % during the first 1.5 hours, *$p < 0.05$. On the other hand, none of the withdrawn samples of rHuKGF-loaded CNPs formulation were exhibited a rHuKGF release within 2 hours in phosphate buffer pH 1.2. After replacing the phosphate buffer pH 1.2 with phosphate buffer pH 5.5, the withdrawn samples started to show rHuKGF cumulative percentage release of 46.9 ± 2.72 % within 2.5 hours and reached 70.1 ± 4.70 % within 4 hours. Finally, with phosphate buffer pH 7.4, the withdrawn samples showed an increase in the amount of rHuKGF released to 74.7 ± 4.08 % after 4.5 hours and reached 89.5 ± 2.77 % within 6 hours, ****$p < 0.0001$. (*A higher resolution / colour version of this figure is available in the electronic copy of the article*).

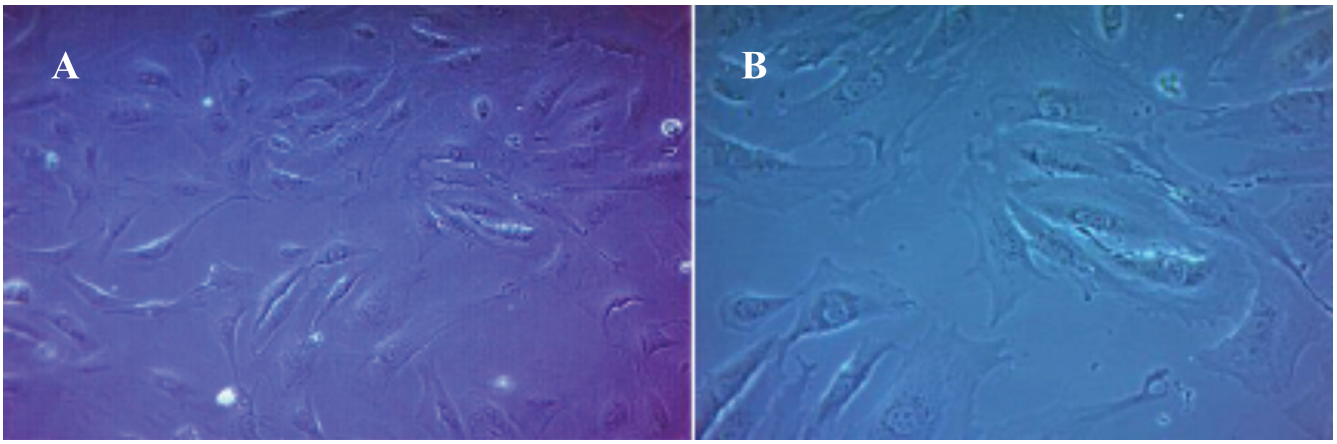

Fig. (2). Light microscope image of FHs 74 Int cells (**A**) 100x, (**B**) 200x. (*A higher resolution / colour version of this figure is available in the electronic copy of the article*).

of the FHs 74 Int cells since a drastic increase of the proliferation rate was observed with the positive control cells, $p < 0.05$. Fluorescence microscope imaging revealed that the FHs 74 Int cellular uptake of rHuKGF-loaded CNPs is time-dependent, (Fig. **4**), (images were taken at 1, 3 and 6 hours incubation time, after repeated washing with PBS). The rhodamine-labelled rHuKGF-loaded CNPs were localized next to the nucleus, this indicates that a portion of the rHuKGF-loaded CNPs were taken up by means of endocytosis and thereby localized inside the cells. The NPs have formed intracellular aggregates, which yielded to a punctuated staining pattern that increased by time, from 1, 3 and 6 hours, Fig. (**4C**, **4F** and **4I**) respectively.

3.6. Animal Studies

Therefore, cellular internalization of the prepared rHuKGF-loaded CNPs was time-dependent and the uptake efficiency was enhanced by mucoadhesive and absorption enhancement properties of chitosan, $p < 0.05$. The endocytosis pathway is the only uptake mechanism by which intracellular lysosomal/phagosomal localization of NPs can be justified [42-44]. On the other hand, no difference observed in the percentage cell viability for cells seeded with CNPs only, Fig. (**3**).

Kollicoat MAE 100 P capsules filled with rHuKGF-loaded CNPs, were developed and optimized for oral delivery

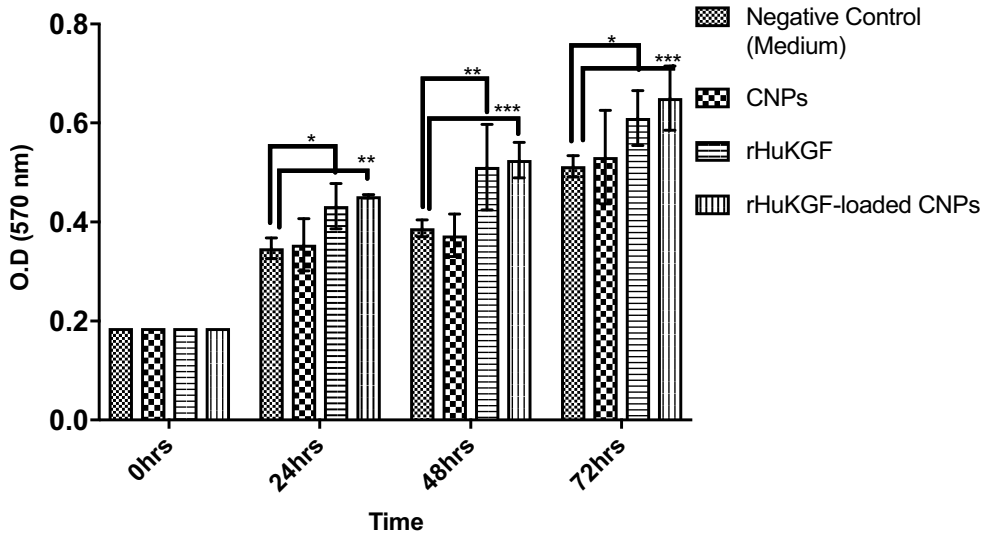

Fig. (3). The viability of FHs 74 Int cells according to MTT assay before and after exposure to rHuKGF-loaded CNPs, rHuKGF and CNPs. (n= 6), where *$p < 0.05$, **$p < 0.01$ and ***$p < 0.001$. (*A higher resolution / colour version of this figure is available in the electronic copy of the article*).

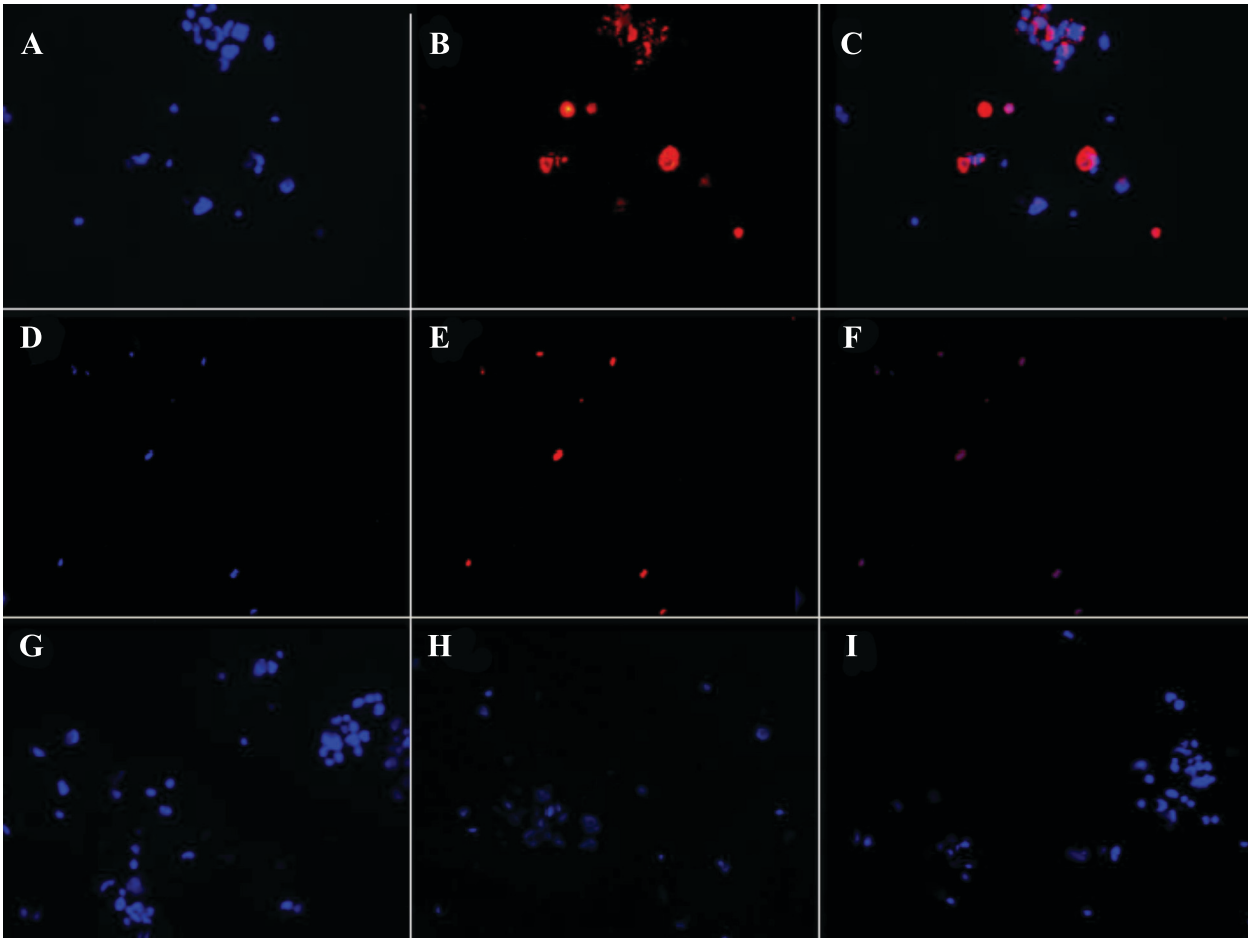

Fig. (4). Fluorescence microscope images (images taken at 400x magnification) show time-dependent FHs 74 Int cellular uptake of rHuKGF-loaded rhodamine-labeled CNPs after 1, 3 and 6 hours incubation time followed by 3x washing with PBS. The cellular uptake after 1 hour incubation presented by images (**A**) FHs 74 Int cells labeled nucleus with DAPI (blue), (**B**) cellular distribution and localization of rHuKGF-loaded rhodamine-labelled CNPs within FHs 74 Int cells (red), (**C**) merged image of A and B. The cellular uptake of rHuKGF-loaded rhodamine-labeled CNPs after 3 hours incubation time presented by images (**D**) FHs 74 Int cells labeled nucleus with DAPI (blue), (**E**) cellular distribution and localization of rHuKGF-loaded rhodamine-labelled CNPs within FHs 74 Int cells (red), (**F**) merged image of D and E. Images (**G**), (**H**) and (**I**) show the cellular uptake after 6 hours incubation time of rhodamine-labeled rHuKGF-loaded CNPs. (*A higher resolution / colour version of this figure is available in the electronic copy of the article*).

Table 2. Pharmacokinetic parameters after intravenous injection of rHuKGF and oral administration of rHuKGF-loaded CNPs given as coated capsules. (mean ± SD, *n*=3)*.

Parameter	IV Administration	Oral Administration
C_{Max} (pg/µL)	328.95 ± 5.21	197.12 ± 2.98
$t_{1/2}$ (hour)	2.5 ± 0.20	11 ± 0.40
$AUC_{(0-\infty)}$ (pg/h/µL)	1452.58 ± 6.22	2461.65 ± 11.08
$AUMC_{(0-\infty)}$ (pg/h/µL)	5082.27 ± 18.94	20672.39 ± 23.47
Cl (L/hour)	0.1342 ± 0.001	0.0772 ± 0.0001
Vd (L)	0.4826 ± 0.0002	1.2359 ± 0.005
%F	100%	69%

*$p < 0.05$.

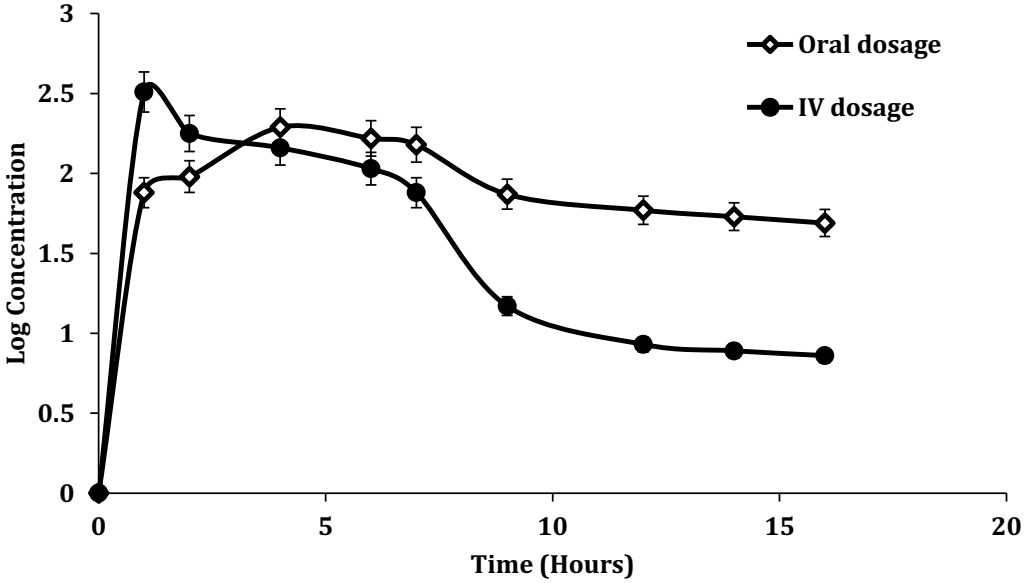

Fig. (5). Serum levels of rHuKGF, are determined at the indicated time points throughout 16 hours after a single dose of 60 µg/kg as IV and oral dosages (mean ± SD, n=3, $p < 0.05$). (*A higher resolution / colour version of this figure is available in the electronic copy of the article*).

of rHuKGF. The mucoadhesive and absorption enhancement properties of chitosan and the protective effect of methacrylic acid-methyl methacrylate copolymer against rHuKGF release into stomach were combined to promote and ensure rHuKGF intestinal absorption [45, 46]. The pH-dependent solubility, swelling and erosion of methacrylic acid-methyl methacrylate copolymer increased as the pH increases. This polymer can dissolve rapidly upon deprotonation of carboxylic acid groups at specific pH values. Wherefore, the release profiles of these NPs exhibited significant pH-sensitivity [47]. It has been reported that microspheres of acrylic acid and methyl methacrylate did not adhere to gastric-mucosa at pH 1.2 but showed mucoadhesion to intestinal mucosa at pH 6.836. Thus, these NPs on oral administration, would release the drug in intestinal, suggesting the potential intestinal targeted drug delivery system. The pharmacokinetic parameters were determined based on the serum rHuKGF levels, following single IV or oral dosages using rabbit as animal model. The rHuKGF exhibited linear pharmacokinetics/ a one-compartment model with first-order kinetics in the dose of 60 µg/kg after single-dose administration. Summary of rHuKGF pharmacokinetic parameters after rHuKGF administration is presented in Table **2**. The IV group exhibited a rapid increase in serum rHuKGF levels up to 328.95 pg/µl over 15 minutes of administration, (Fig. **5**). Whereas, the oral administration of rHuKGF-loaded CNPs exhibited slower absorption and sustained elimination, reaching a maximum serum rHuKGF levels after 4 hours (197.12 pg/µl). Ideally, this delay can be explained as rHuKGF remains associated with CNPs in gastric conditions, and it is only released at the intestinal pH where the absorption potential is optimal [48, 49]. Following a pH change to ≥ 5.5, a rapid release pattern was observed, characterized by a release during the first hour, (Fig. **5**). The elimination of the IV dose was rapid when compared to the oral dose, with terminal $t_{1/2}$ of 2.4 hours and 11 hours respectively. Moreover, the serum rHuKGF levels of the oral group were significantly different from that of the IV group $P < 0.05$. The AUC of orally administered NPs was 2461.65 pg/h/µL and 1452.58 pg/h/µL for the IV dose. The median AUC to infinity was 20672.39±23.47 (pg/h/µL) for oral administration and 5082.27±18.94 (pg/h/µL) for IV administration. The corresponding absolute bioavailability for the oral dose was calculated to be 69%. The serum levels of rHuKGF detected

initially following the oral dose as seen in Fig. (**5**), revealed that the absorption of rHuKGF was to a higher extent from the developed NPs. Subsequent continuous absorption of rHuKGF, over 4 hours, is due to the ongoing sustained release of rHuKGF during NPs adhesion to the intestinal mucosa, and mainly due to the passage of NPs to the posterior small intestine, contributing to the serum level of rHuKGF. Despite mucoadhesive properties, CNPs slide along the intestine maintaining their physical structure. In fact, chitosan-based NPs have shown mucoadhesive capacities *in-vitro*, and concomitant slow upper small intestinal transit *in-vivo*, but this intestinal retention was limited to a few hours [43, 50]. The arrival of CNPs to the posterior intestine occurs in a few hours, and due to the maintained adhesive properties, uptake is promoted [51, 52]. The prepared CNPs appeared to stabilize and protect entrapped rHuKGF from degradation in the GIT, as rHuKGF was detected in high concentration in serum following the oral administration.

CONCLUSION

The study revealed that the physicochemical characteristics of the chitosan-based NPs have promoted oral administration of rHuKGF–loaded NPs filled in methacrylic acid-methyl methacrylate copolymer-coated capsules and it is practically alternative to the IV route since the absolute bioavailability of orally administered rHuKGF–loaded CNPs, using rabbit as animal model, was 69%. The study explained the systemic exposure of rHuKGF by AUC of oral dosage when compared to IV dosage. Fluorescence microscope imaging revealed that the FHs 74 Int cellular uptake of rHuKGF-loaded CNPs is time-dependent, followed by significant increase in the percentage cell viability.

ETHICS APPROVAL AND CONSENT TO PARTICIPATE

The approval of the ethics committee of Faculty Research and Scholarly Activity (FRSA), Faculty of Pharmaceutical Sciences, UCSI University Animal Care and Use Committee (Ref: UCSI/Pharmacy/2014/FRGS/Approval/01).

HUMAN AND ANIMAL RIGHTS

No human were used in this study. All animal related experiments are in accordance with the standards set forth in the 8th Edition of *Guide for the Care and Use of Laboratory Animals* (http:// grants.nih.gov/grants/olaw/Guide for the-care-and-use-of-laboratory-animals.pdf) published by the National Academy of Sciences, The National Academies Press, Washington DC, United States of America.

CONSENT FOR PUBLICATION

Not applicable.

AVAILABILITY OF DATA AND MATERIALS

Not applicable.

FUNDING

This study was supported by a grant from the Ministry of Higher Education (MOHE) through the Fundamental Research Grant Scheme (Ref: FRGS/2/2014/SKK02/UCSI/02/1), Malaysia.

CONFLICT OF INTEREST

The authors declare no conflict of interest, financial or otherwise.

ACKNOWLEDGMENT

Declared none.

REFERENCES

[1] Hattori Y, Yamasaki M, Konishi M, Itoh N. Spatially restricted expression of fibroblast growth factor-10 mRNA in the rat brain. Brain Res Mol Brain Res 1997; 47(1-2): 139-46. [http://dx.doi.org/10.1016/S0169-328X(97)00044-2] [PMID: 9221911]

[2] Ohuchi H, Nakagawa T, Yamamoto A, *et al.* The mesenchymal factor, FGF10, initiates and maintains the outgrowth of the chick limb bud through interaction with FGF8, an apical ectodermal factor. Development 1997; 124(11): 2235-44. [PMID: 9187149]

[3] Guo L, Degenstein L, Fuchs E. Keratinocyte growth factor is required for hair development but not for wound healing. Genes Dev 1996; 10(2): 165-75. [http://dx.doi.org/10.1101/gad.10.2.165] [PMID: 8566750]

[4] Park JW, Hwang SR, Yoon IS. Advanced Growth Factor De-livery Systems in Wound Management and Skin Regeneration. Molecules 2017; 22: 1259. [http://dx.doi.org/10.3390/molecules22081259]

[5] Kitsberg DI, Leder P. Keratinocyte growth factor induces mammary and prostatic hyperplasia and mammary adenocarcinoma in transgenic mice. Oncogene 1996; 13(12): 2507-15. [PMID: 9000125]

[6] Finch PW, Mark Cross LJ, McAuley DF, Farrell CL. Palifermin for the protection and regeneration of epithelial tissues following injury: new findings in basic research and pre-clinical models. J Cell Mol Med 2013; 17(9): 1065-87. [http://dx.doi.org/10.1111/jcmm.12091] [PMID: 24151975]

[7] Ishikawa A, Kudo M, Nakazawa N, *et al.* Expression of keratinocyte growth factor and its receptor in human endometrial cancer in cooperation with steroid hormones. Int J Oncol 2008; 32(3): 565-74. [http://dx.doi.org/10.3892/ijo.32.3.565] [PMID: 18292933]

[8] Beaven AW, Shea TC. Recombinant human keratinocyte growth factor palifermin reduces oral mucositis and improves patient outcomes after stem cell transplant. Drugs Today (Barc) 2007; 43(7): 461-73. [http://dx.doi.org/10.1358/dot.2007.43.7.1119723] [PMID: 17728847]

[9] Blijlevens N, Sonis S. Palifermin (recombinant keratinocyte growth factor-1): a pleiotropic growth factor with multiple biological activities in preventing chemotherapy- and radiotherapy-induced mucositis. Ann Oncol 2007; 18(5): 817-26. [http://dx.doi.org/10.1093/annonc/mdl332] [PMID: 17030544]

[10] Morris J, Rudebeck M, Neudorf S, *et al.* Safety, pharmacoki-netics, and efficacy of palifermin in children and adolescents with acute leukemias undergoing myeloablative therapy and allogeneic hematopoietic stem cell transplantation: a pediatric blood and marrow transplant consortium trial. Biol Blood Marrow Transplant 2016; 22(7): 1247-56. [http://dx.doi.org/10.1016/j.bbmt.2016.02.016] [PMID: 26968792]

[11] Pinakini K, Bairy K. Palifermin: A keratinocyte growth factor for oral mucositis. Indian J Pharmacol 2005; 37(5): 338. [http://dx.doi.org/10.4103/0253-7613.16865]

[12] Gullotti E, Yeo Y. Extracellularly activated nanocarriers: a new paradigm of tumor targeted drug delivery. Mol Pharm 2009; 6(4): 1041-51. [http://dx.doi.org/10.1021/mp900090z] [PMID: 19366234]

[13] Hobbs SK, Monsky WL, Yuan F, *et al.* Regulation of transport pathways in tumor vessels: role of tumor type and microenvironment. Proc Natl Acad Sci USA 1998; 95(8): 4607-12. [http://dx.doi.org/10.1073/pnas.95.8.4607] [PMID: 9539785]

[14] Sun M, Sun B, Liu Y, Shen QD, Jiang S. Dual-color fluores-cence imaging of magnetic nanoparticles in live cancer cells using conjugated polymer probes. Sci Rep 2016; 6: 22368. [http://dx.doi.org/10.1038/srep22368] [PMID: 26931282]

[15] Nishimori H, Kondoh M, Isoda K, Tsunoda S, Tsutsumi Y, Yagi K. Silica nanoparticles as hepatotoxicants. Eur J Pharm Biopharm 2009; 72(3): 496-501. [http://dx.doi.org/10.1016/j.ejpb.2009.02.005] [PMID: 19232391]

[16] Moser F, Hildenbrand G, Müller P, *et al.* Cellular uptake of gold nanoparticles and their behavior as labels for localization microscopy. Biophys J 2016; 110(4): 947-53. [http://dx.doi.org/10.1016/j.bpj.2016.01.004] [PMID: 26910431]

[17] Shang L, Nienhaus K, Jiang X, *et al.* Nanoparticle interactions with live cells: Quantitative fluorescence microscopy of nanoparticle size effects. Beilstein J Nanotechnol 2014; 5: 2388-97. [http://dx.doi.org/10.3762/bjnano.5.248] [PMID: 25551067]

[18] Maeda H. The enhanced permeability and retention (EPR) effect in tumor vasculature: the key role of tumor-selective macromolecular drug targeting. Adv Enzyme Regul 2001; 41(1): 189-207. [http://dx.doi.org/10.1016/S0065-2571(00)00013-3] [PMID: 11384745]

[19] Chang SJ, Niu GC, Kuo SM, Chen SF. Preparation and preliminary characterization of concentric multi-walled chitosan microspheres. J Biomed Mater Res A 2007; 81(3): 554-66. [http://dx.doi.org/10.1002/jbm.a.31084] [PMID: 17133452]

[20] Wang JJ, Zeng ZW, Xiao RZ, *et al.* Recent advances of chitosan nanoparticles as drug carriers. Int J Nanomedicine 2011; 6: 765-74. [PMID: 21589644]

[21] Cao JN, Zhou J. Progress in antitumor studies of chitosan. Chin J Biochem Pharm 2005; 26(2): 127-37.

[22] Xia G, Liu Y, Tian M, *et al.* Nanoparticles/thermosensitive hydrogel reinforced with chitin whiskers as a wound dressing for treating chronic wounds. J Mater Chem 2017; 5(17): 3172-85. [http://dx.doi.org/10.1039/C7TB00479F]

[23] Hans ML, Lowman AM. Biodegradable nanoparticles for drug delivery and targeting. Curr Opin Solid State Mater Sci 2002; 6(4): 319-27. [http://dx.doi.org/10.1016/S1359-0286(02)00117-1]

[24] Pan Y, Li YJ, Zhao HY, *et al.* Bioadhesive polysaccharide in protein delivery system: chitosan nanoparticles improve the intestinal absorption of insulin in vivo. Int J Pharm 2002; 249(1-2): 139-47. [http://dx.doi.org/10.1016/S0378-5173(02)00486-6] [PMID: 12433442]

[25] Calvo P, Remuñan-López C, Vila-Jato JL, Alonso MJ. Chitosan and chitosan/ethylene oxide-propylene oxide block copolymer nanoparticles as novel carriers for proteins and vaccines. Pharm Res 1997; 14(10): 1431-6. [http://dx.doi.org/10.1023/A:1012128907225] [PMID: 9358557]

[26] Fan W, Yan W, Xu Z, Ni H. Formation mechanism of monodisperse, low molecular weight chitosan nanoparticles by ionic gelation technique. Colloids Surf B Biointerfaces 2012; 90: 21-7. [http://dx.doi.org/10.1016/j.colsurfb.2011.09.042] [PMID: 22014934]

[27] Lee MK, Kim MY, Kim S, Lee J. Cryoprotectants for freeze drying of drug nano-suspensions: effect of freezing rate. J Pharm Sci 2009; 98(12): 4808-17. [http://dx.doi.org/10.1002/jps.21786] [PMID: 19475555]

[28] Varshosaz J, Eskandari S, Tabbakhian M. Freeze-drying of nanostructure lipid carriers by different carbohydrate poly-mers used as cryoprotectants. Carbohydr Polym 2012; 88(4): 1157-63. [http://dx.doi.org/10.1016/j.carbpol.2012.01.051]

[29] Zhang HL, Wu SH, Tao Y, Zang LQ, Su ZQ. Preparation and characterization of water-soluble chitosan nanoparticles as protein delivery system. J Nanomater 2010; 1. [http://dx.doi.org/10.1155/2010/898910]

[30] KGF (FGF-7) Human SimpleStep ELISA® Kit. In: abcam, editor. 2016.

[31] Lachman L, Lieberman HA, Kanig JL. The theory and prac-tice of industrial pharmacy. Philadelphia: Lea & Febiger 1976.

[32] Cole ET, Scott RA, Connor AL, *et al.* Enteric coated HPMC capsules designed to achieve intestinal targeting. Int J Pharm 2002; 231(1): 83-95. [http://dx.doi.org/10.1016/S0378-5173(01)00871-7] [PMID: 11719017]

[33] Mosmann T. Rapid colorimetric assay for cellular growth and survival: application to proliferation and cytotoxicity assays. J Immunol Methods 1983; 65(1-2): 55-63. [http://dx.doi.org/10.1016/0022-1759(83)90303-4] [PMID: 6606682]

[34] van de Loosdrecht AA, Beelen RH, Ossenkoppele GJ, Broekhoven MG, Langenhuijsen MM. A tetrazolium-based colorimetric MTT assay to quantitate human monocyte mediated cytotoxicity against leukemic cells from cell lines and patients with acute myeloid leukemia. J Immunol Methods 1994; 174(1-2): 311-20. [http://dx.doi.org/10.1016/0022-1759(94)90034-5] [PMID: 8083535]

[35] Ferrari M, Fornasiero MC, Isetta AM. MTT colorimetric assay for testing macrophage cytotoxic activity in vitro. J Immunol Methods 1990; 131(2): 165-72. [http://dx.doi.org/10.1016/0022-1759(90)90187-Z] [PMID: 2391427]

[36] Gerlier D, Thomasset N. Use of MTT colorimetric assay to measure cell activation. J Immunol Methods 1986; 94(1-2): 57-63. [http://dx.doi.org/10.1016/0022-1759(86)90215-2] [PMID: 3782817]

[37] Scudiero DA, Shoemaker RH, Paull KD, *et al.* Evaluation of a soluble tetrazolium/formazan assay for cell growth and drug sensitivity in culture using human and other tumor cell lines. Cancer Res 1988; 48(17): 4827-33. [PMID: 3409223]

[38] Chitra K, Annadurai G. Synthesis and characterization of dye coated fluorescent chitosan nanoparticles. J Acad Ind Res 2012; 15: 199. [http://dx.doi.org/10.3390/ijms160920943] [PMID: 26340627]

[39] Palanirajan VK, Marwan AM, Mhd LT, Yeong SW, Lee MT, Abu Bakar BM. Detection of Formation of Recombinant Hu-man Keratinocyte Growth Factor Loaded Chitosan Nanoparti-cles Based on its Optical Properties. Curr Nanosci 2018; 14(2): 127-35. [http://dx.doi.org/10.2174/1573413713666171016150707]

[40] Palanirajan VK, Marwan AM, Lee MT, Yeong SW, Abu Bakar BM, Eds. UV-spectroscopy Method for Detecting the Chi-tosan Nanoparticles Formation. Proceedings of the Interna-tional Conference of Applied Nanotechnology and Nanoscience 2017 Oct 18-20; Rome, Italy. 293.

[41] Konturek SJ, Brzozowski T, Konturek JW, Slomiany BL. Growth factors in gastric mucosal integrity, protection and healing of acute and chronic ulcerations.In The stomach 1993; pp. 159-76. [http://dx.doi.org/10.1007/978-3-642-78176-6_11]

[42] Qian Z, Dougherty PG, Pei D. Targeting intracellular protein-protein interactions with cell-permeable cyclic peptides. Curr Opin Chem Biol 2017; 38: 80-6. [http://dx.doi.org/10.1016/j.cbpa.2017.03.011] [PMID: 28388463]

[43] Wang T, Wang L, Li X, *et al.* Size-dependent regulation of intracellular trafficking of polystyrene nanoparticle-based drug delivery carriers. ACS Appl Mater Interfaces 2017; 9(22): 18619-25. [http://dx.doi.org/10.1021/acsami.7b05383] [PMID: 28497682]

[44] MacParland SA, Tsoi KM, Ouyang B, *et al.* Phenotype deter-mines nanoparticle uptake by human macrophages from liver and blood. ACS Nano 2017; 11(3): 2428-43. [http://dx.doi.org/10.1021/acsnano.6b06245] [PMID: 28040885]

[45] Liang J, Yan H, Puligundla P, Gao X, Zhou Y, Wan X. Applications of chitosan nanoparticles to enhance absorption and bioavailability of tea polyphenols: A review. Food Hydrocoll 2017; 69: 286-92. [http://dx.doi.org/10.1016/j.foodhyd.2017.01.041]

[46] Patra CN, Priya R, Swain S, Jena GK, Panigrahi KC, Ghose D. Pharmaceutical significance of Eudragit: A review. Future J Pharm Sci 2017; 3(1): 33-45. [http://dx.doi.org/10.1016/j.fjps.2017.02.001]

[47] Dai J, Nagai T, Wang X, Zhang T, Meng M, Zhang Q. pH-sensitive nanoparticles for improving the oral bioavailability of cyclosporine A. Int J Pharm 2004; 280(1-2): 229-40. [http://dx.doi.org/10.1016/j.ijpharm.2004.05.006] [PMID: 15265562]

[48] Kumar J, Newton AMJ. Rifaximin - Chitosan Nanoparticles for Inflammatory Bowel Disease (IBD). Recent Pat Inflamm Allergy Drug Discov 2017; 11(1): 41-52. [http://dx.doi.org/10.2174/1872213X10666161230111226] [PMID: 28034350]

[49] Li L, Jiang G, Yu W, *et al.* Preparation of chitosan-based multifunctional nanocarriers overcoming multiple barriers for oral delivery of insulin. Mater Sci Eng C 2017; 70(Pt 1): 278-86. [http://dx.doi.org/10.1016/j.msec.2016.08.083] [PMID: 27770892]

[50] Banerjee A, Lee J, Mitragotri S. Intestinal mucoadhesive devices for oral delivery of insulin. Bioeng Transl Med 2016; 1(3): 338-46. [http://dx.doi.org/10.1002/btm2.10015] [PMID: 29313019]

[51] Yin L, Wang Y, Wang C, Feng M. Nano-reservoir Bioadhesive Tablets Enhance Protein Drug Permeability Across the Small Intestine. AAPS PharmSciTech 2017; 18(6): 2329-35. [http://dx.doi.org/10.1208/s12249-016-0709-6] [PMID: 28116599]

[52] Zhang J, Zhu X, Jin Y, Shan W, Huang Y. Mechanism study of cellular uptake and tight junction opening mediated by goblet cell-specific trimethyl chitosan nanoparticles. Mol Pharm 2014; 11(5): 1520-32. [http://dx.doi.org/10.1021/mp400685v] [PMID: 24673570]